

Article

Developing Multicompartment Biopolymer Hydrogel Beads for Tandem Chemoenzymatic One-Pot Process

Jan Pauly ^{1,2} , Harald Gröger ²  and Anant V. Patel ^{1,*} 

¹ WG Fermentation and Formulation of Biologicals and Chemicals, Faculty of Engineering Sciences and Mathematics, Bielefeld University of Applied Sciences, Interaktion 1, 33619 Bielefeld, Germany; jan.pauly@fh-bielefeld.de

² Chair of Organic Chemistry I, Faculty of Chemistry, Bielefeld University, Universitätsstrasse 25, 33615 Bielefeld, Germany; harald.groeger@uni-bielefeld.de

* Correspondence: anant.patel@fh-bielefeld.de

Received: 28 May 2019; Accepted: 15 June 2019; Published: 18 June 2019



Abstract: Chemoenzymatic processes have been gaining interest to implement sustainable reaction steps or even create new synthetic routes. In this study, we combined Grubbs' second-generation catalyst with pig liver esterase and conducted a chemoenzymatic one-pot process in a tandem mode. To address sustainability, we encapsulated the catalysts in biopolymer hydrogel beads and conducted the reaction cascade in an aqueous medium. Unfortunately, conducting the process in tandem led to increased side product formation. We then created core-shell beads with catalysts located in different compartments, which notably enhanced the selectivity towards the desired product compared to homogeneously distributing both catalysts within the matrix. Finally, we designed a specific large-sized bead with a diameter of 13.5 mm to increase the diffusion route of the Grubbs' catalyst-containing shell. This design forced the ring-closing metathesis to occur first before the substrate could diffuse into the pig liver esterase-containing core, thus enhancing the selectivity to 75%. This study contributes to addressing reaction-related issues by designing specific immobilisates for chemoenzymatic processes.

Keywords: chemoenzymatic; multicompartment; biopolymer; encapsulation; one-pot; tandem

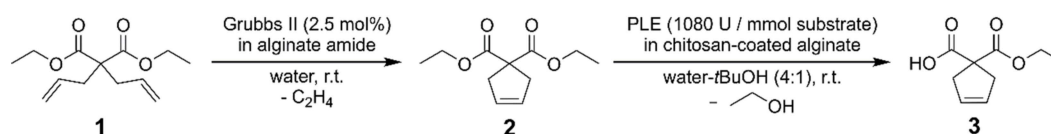
1. Introduction

Sustainability in chemistry has been developing into an expanding and complex field due to increasing demand in recent years [1,2]. There are different approaches to address this topic such as using water as reaction medium [3], enabling catalyst recycling [4], implementing more sustainable reaction steps in synthesis routes or even starting from renewable resources and creating new synthesis routes [5]. Since chemical processes in industry often imply catalytic reaction steps, it is of major interest to develop new catalytic processes with catalysts that are highly selective, stable and catalyse reactions at mild conditions.

One option to meet these requirements is the implementation of biocatalysts in organic synthesis since enzymes are often highly selective and the reactions can be conducted in water using mild reaction conditions [6–8]. Such biotransformations are often complementary to the tools of chemocatalysis, which themselves are suitable for reactions not being able to be conducted by enzymes. Therefore, the development of new catalytic processes featuring both chemo- and biocatalysis has increasingly been reported in recent years [9–14]. Those reports feature the combination of enzymes with metal- or organocatalysts, with reaction sequences conducted either in a classical sequential way or in tandem [15–26].

However, as in most of the studies with a chemoenzymatic approach non-immobilised catalysts were used, the opportunity of catalyst recycling for achieving a more improved overall process was often overlooked. Immobilisation can enhance stability and recyclability of catalysts as well as it can contribute to overcoming compatibility issues by compartmentation when using multiple catalysts together [27–31]. One suitable method for immobilisation addressing sustainability is encapsulation in biopolymer hydrogels as renewable resources. Using these materials for encapsulating enzymes has been reported for a long time [32–39], whereas for chemocatalysts there are only few reports covering that topic [40–44].

Previously, we reported a chemoenzymatic one-pot reaction sequence featuring a ring-closing metathesis (RCM) followed by enzymatic ester hydrolysis (EEH) conducted by a bio- and a chemocatalyst both encapsulated in biopolymer-based hydrogels (Scheme 1) [45]. This reaction sequence is based on a previous report, in which both catalysts were used non-encapsulated, and the process was conducted sequentially [46]. In our previous study, we conducted the RCM in water with Grubbs' second-generation catalyst encapsulated in octyl-grafted alginate amide and the EEH in water-*t*BuOH (4:1) with pig liver esterase (PLE) encapsulated in chitosan-coated alginate, with the reaction process conducted sequentially.



Scheme 1. Studied chemoenzymatic one-pot process featuring ring-closing metathesis and enzymatic ester hydrolysis.

In this consecutive study, we now aimed for conducting the reaction sequence in a tandem mode. Since in our previous study we revealed that encapsulating the catalysts enabled their compatibility, we now investigated whether the tandem reaction is feasible using encapsulated catalysts. Our starting point is based on our previous study using octyl-grafted alginate amide and chitosan-coated alginate as the most suitable encapsulation matrices. Since in this setup both catalysts are present right from the beginning and shielding of the catalysts is essential, we further investigated the influence of the matrix on the reactions. For this, we examined catalysts encapsulated in different beads as well as co-encapsulated in the same bead and investigated the influence of catalyst compartmentation.

2. Results and Discussion

2.1. Benchmark

Conducting the reaction sequence in tandem implies that the enzyme is present from the beginning. Therefore, substrate 1 can be hydrolysed instead of or additionally to the desired ring-closing product 2, leading to the undesired side product 4 (Figure 1b). We aimed at evaluating the extent of the side reaction and set the benchmarks for both enzymatic reactions in our initial study by conducting the reactions with PLE being non-encapsulated and encapsulated in chitosan-coated alginate and determining the initial reaction rates (Figure 1).

First, we used water as reaction medium, which had been revealed as most suitable medium for the RCM in our previous study, and found that with non-encapsulated PLE the side reaction with 1.340 $\mu\text{mol}/\text{min}$ was significantly slower than the desired reaction but still much faster than the RCM with encapsulated catalyst at the same reaction conditions (0.333 $\mu\text{mol}/\text{min}$) [47]. Since the side reaction was kinetically favoured over the RCM, this would suppress the desired enzymatic reaction. Encapsulating the enzyme led to reduced reaction rates for both reactions, lowering the side reaction rate to 0.287 $\mu\text{mol}/\text{min}$, which is at the same level as for the RCM and therefore still too

high. Then, we conducted the reaction in water-*t*BuOH (4:1), which turned out to be the most suitable medium for the EEH in our previous study, and found that both reactions were notably suppressed, in particular by using encapsulated enzyme. It should be noted that using this reaction medium instead of water is mandatory since it is known that without co-solvent the desired product **3** can undergo a decarboxylation, which we also observed [46,48,49]. Though the RCM with encapsulated catalyst was very slow in this medium (0.056–0.118 $\mu\text{mol}/\text{min}$) [45], we chose to continue our study with this medium in order to suppress the side reaction and avoid product decarboxylation.

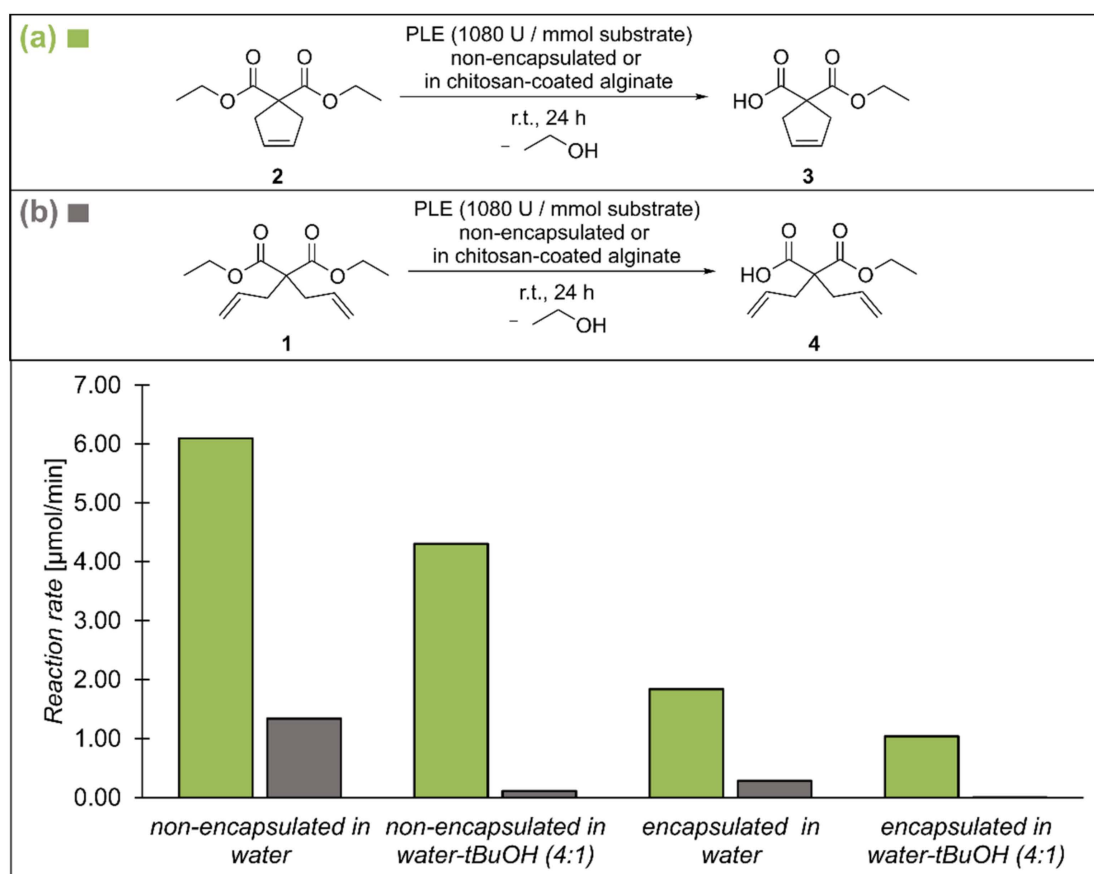


Figure 1. Benchmark enzymatic ester hydrolysis revealed higher reaction rates for desired reaction ((a), green) than for side reaction ((b), grey) in different reaction media.

2.2. Separate Encapsulation

After we had set the benchmark and selected water-*t*BuOH (4:1) as a suitable solvent, we investigated the tandem reaction using non-encapsulated catalysts and catalysts encapsulated in separate beads (Table 1). For both non-encapsulated catalysts (entry 1) we found a low selectivity of 18% and 57% total conversion. With the Grubbs' catalyst being encapsulated and PLE being non-encapsulated (entry 2), selectivity dropped to 1% due to notably lowered RCM reaction rate, which is in line with our previous studies [45,47]. At the same time, due to the non-encapsulated PLE (entry 2), the side reaction was favoured with an almost quantitative conversion. In contrast, encapsulating only PLE (entry 3) notably enhanced the selectivity to 50% due to reduced enzyme activity and high Grubbs' activity while lowering the conversion. Consequently, encapsulating both catalysts (entry 4) notably reduced selectivity below 1% and conversion to 50%, which is in line with the previous results.

Table 1. Encapsulating the catalysts in separate beads influenced the selectivity.

Entry	Grubbs' Catalyst/PLE	Selectivity (Main Product 3) [%]	Conversion [%]	Initial Overall Reaction Rate [$\mu\text{mol}/\text{min}$]
1	Non-encapsulated/non-encapsulated	18	57	0.137
2	Alginate amide/non-encapsulated	1	95	0.201
3	Non-encapsulated/chitosan-coated alginate	50	64	0.204
4	Alginate amide/chitosan-coated alginate	<1	50	0.060

Grubbs' catalyst: 2.5 mol%, PLE: 1080 U/mmol substrate, 0.25 mmol substrate, r.t., 72 h.

Due to the low selectivities when using both catalysts encapsulated separately, we deliberated different approaches to address this issue. One approach to optimise the reaction could comprise using a more suitable PLE isoenzyme, since the crude PLE consists of several isoenzymes [50]. It has been reported that these isoenzymes do not only differ in enantioselectivity but also in substrate selectivity [51–54]. Hence, screening the different isoenzymes could result in finding a more substrate selective PLE for our system. Since in this proof of concept study we aimed at designing a new formulation system for the catalysts to improve the selectivity, we did not address the approach of changing the enzymatic system. Another idea towards a more selective reaction process is to adjust both reactions' rates, more precisely accelerating the RCM and decelerating the EEH. However, even with this approach, when using catalysts encapsulated in separate beads, substrate 1 could still randomly diffuse into enzyme beads first instead of the Grubbs' beads, which should be avoided. Since in this study we focused on investigating the influence of encapsulation on the reaction, we chose the approach of designing specific beads to suppress the side reaction and gain more insights into the influence of compartmentation.

2.3. Co-Encapsulation

In more detail, our approach was to co-encapsulate both catalysts in one bead and enforce the proper reaction sequence by catalyst compartmentation. First, we confirmed the selectivity issue by co-encapsulating both catalysts distributed homogeneously in different matrices. To accelerate the ring-closing metathesis, we increased the Grubbs' catalyst loading to 10 mol% (compared to 2.5 mol% used before). The beads consisted of either calcium alginate, chitosan-coated alginate or octyl-grafted alginate amide and revealed similar reaction rates, high conversions of 94–98% but very low selectivities of 1–7% (Table 2, entries 1–3).

Since this was in line with the results of separately encapsulated catalysts, we then developed beads with catalysts located in different compartments. As encapsulation matrix for PLE, we chose cross-linked chitosan, which acted as the best material in terms of leaching and provided less enzyme activity than chitosan-coated alginate beads in our previous study [55], which in this case is desired to decrease the enzymatic reaction. We then coated these beads, having a diameter of 2.6 mm, with octyl-grafted alginate amide for Grubbs' catalyst encapsulation multiple times to get core-shell beads with Grubbs' catalyst located in between the alginate amide layers (Scheme 2).

Each alginate amide layer had an average thickness of 0.5 mm, leading to a total bead diameter growing of approx. 1 mm per layer. The first multicompartments beads with a diameter of 5.0 mm had three shell layers of Grubbs' catalyst-containing alginate amide and gave a selectivity of 32%, which already is a great improvement compared to separately encapsulated catalysts (Table 2, entry 4, Figure A1a). Unfortunately, the overall reaction rate dropped to 0.026 $\mu\text{mol}/\text{min}$. Nevertheless, we continued with this type of beads and reduced the amount of enzyme by 60% to decrease the side reaction, which enhanced selectivity only slightly to 35% (Table 2, entry 5). Therefore, we increased the diffusion route for the RCM by adding more Grubbs' catalyst-containing alginate amide layers and additionally crushed the Grubbs' catalyst into smaller particles with a spatula for better distribution.

Applying five alginate amide layers to obtain beads with a diameter of 6.2 mm resulted in higher residence time in this shell for substrate **1**, thus enhancing the selectivity to 44% (Table 2, entry 6). Next, we applied seven alginate amide layers (final bead diameter: 8.9 mm) to raise the selectivity to 56% (Table 2, entry 7). All beads remained intact after the reaction, thus no Grubbs' leaching during reaction occurred.

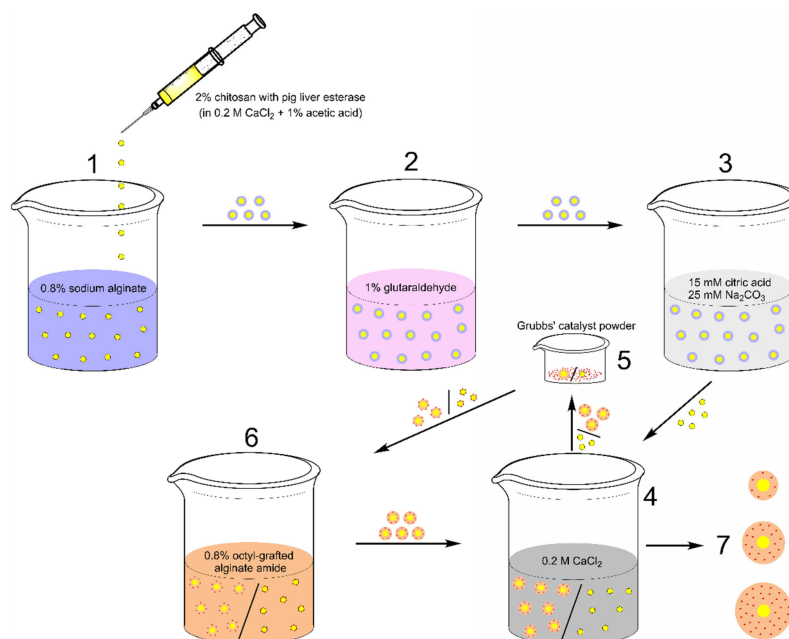
Table 2. Co-encapsulated catalysts in multicompartment beads enhanced the selectivity. Further enhancement was achieved by increasing the bead diameter.

Entry	Bead Type	Selectivity (Main Product) [%]	Conversion [%]	Initial Overall Reaction Rate [$\mu\text{mol}/\text{min}$]
1	Alginate ¹	1	98	0.113
2	Chitosan-coated alginate ¹	7	>99	0.103
3	Alginate amide ¹	1	94	0.094
4	Shell of alginate amide (Grubbs' catalyst) + core of chitosan (PLE) ^{2,3}	32	92	0.026
5	Shell of alginate amide (Grubbs' catalyst) + core of chitosan (PLE) ^{2,3,4}	35	55	0.017
6	Shell of alginate amide (Grubbs' catalyst) + core of chitosan (PLE) ^{2,5,6}	44	74	0.021
7	Shell of alginate amide (Grubbs' catalyst) + core of chitosan (PLE) ^{2,6,7}	56	62	0.026
8	Shell of alginate amide (Grubbs' catalyst) + core of chitosan (PLE) ^{2,6,8}	75	84	0.034

Grubbs' catalyst: 10 mol%, PLE: 1080 or 432 U/mmol substrate, 0.25 mmol substrate, r.t., 168 h. ¹ both catalysts were distributed homogeneously in the matrix. ² beads with catalysts located in different compartments. ³ three shell layers of alginate amide containing Grubbs' catalyst. ⁴ reduced amount of enzyme (−60%). ⁵ five shell layers of alginate amide containing Grubbs' catalyst. ⁶ reduced amount of enzyme (−60%), Grubbs' catalyst crushed. ⁷ seven shell layers of alginate amide containing Grubbs' catalyst. ⁸ twelve shell layers of alginate amide containing Grubbs' catalyst.

We wanted to create even larger beads, but with increasing bead size the concentration of Grubbs' catalyst inside the alginate amide shell would be lowered, when working with a fixed catalyst loading of 10 mol%. Therefore, we produced one bead for our next experiment with twelve layers of alginate amide to concentrate the whole amount of Grubbs' catalyst in one bead (Figure A1b–d). We obtained one large-sized bead with a diameter of 13.5 mm, which we used in our chemoenzymatic process and achieved a selectivity of 75% (Table 2, entry 8).

The overall reaction rates achieved with the core-shell beads (entries 4–8) were all in the same order of magnitude. Limitation of the overall reaction rate is mainly determined by the amount of Grubbs' catalyst inside the shell and the diffusion of the substrate inside the beads. When we applied more shell layers, the diffusion limitation was increased. We compensated this by producing fewer beads and thereby concentrating the overall same amount of Grubbs' catalyst in the reduced number of beads. This compensation led to very similar reaction rates in the range of 0.017–0.034 $\mu\text{mol}/\text{min}$. Though these reaction rates using co-encapsulated catalysts were notably low and should be improved in subsequent studies, we showed in this proof of concept that compartmentation and specific bead design can contribute to suppressing a side reaction and thus enhancing the selectivity towards the desired product.



Scheme 2. Schematic procedure for creating multicompartiment beads: 1. Creating liquid chitosan beads with formative calcium alginate shell. 2. Cross-linking in glutaraldehyde for 20 h to get solid chitosan beads. 3. Dissolving the calcium alginate shell. 4. Stirring in CaCl_2 solution for sufficient Ca^{2+} concentration inside the beads. 5. Rolling the beads in a defined amount of Grubbs' catalyst powder. 6. Adding the beads to alginate amide solution to fix the catalyst and create a layer. Then again stirring the beads in CaCl_2 solution for sufficient Ca^{2+} concentration in next layering step. 7. Repeating steps 4–6 until beads with a desired number of shell layers containing Grubbs' catalyst were obtained.

3. Materials and Methods

3.1. General

All commercially available chemicals were used without further purification. Substance **1** was obtained from Alfa Aesar (Karlsruhe, Germany), Grubbs' second-generation catalyst was obtained from abcr GmbH (Karlsruhe, Germany), PLE was obtained from Sigma-Aldrich (Taufkirchen, Germany) and sodium alginate (Manugel[®] GMB) was obtained from FMC BioPolymer UK (Girvan, United Kingdom). Diethyl cyclopent-3-ene-1,1-dicarboxylate (**2**) was synthesised according to a reported procedure [46], as well as octyl-grafted alginate amide [56]. Both preparations are described in the Supplementary Materials. The overall reaction rates derived from conversions of substrate **1** and pH compensation for the enzymatic hydrolysis reactions were measured respectively controlled by an automated titration (Titroline[®] 7000, SI Analytics, Mainz, Germany) with NaOH solution (0.2 M). Determining the selectivities was done by HPLC analysis on a Macherey-Nagel NUCLEODUR[®] C₁₈ Gravity-SB (5 μm) column. Further information on HPLC analysis is given in the Supplementary Materials. Bead diameters were measured with a calliper ruler.

3.2. Encapsulation Procedures

3.2.1. Preparation of Octyl-Grafted Alginate Amide Beads containing Catalyst/s

Beads were prepared according to the previously reported procedure [47]: Grubbs' second-generation catalyst (6.25 μmol , 5.31 mg or 25 μmol , 21.22 mg) was immobilised using the method of encapsulation. For experiments requiring co-encapsulated catalysts, pig liver esterase (270 U, 15 mg) was added. The catalyst/s was/were suspended in octyl-grafted alginate amide solution (2.5 mL, 2% w/w in H_2O). To reduce the particle size of non-water-soluble Grubbs' catalyst, the catalyst particle aggregates were crushed with a spatula. Then, the suspension was stirred at 500 rpm for 10 min at room temperature

to ensure homogeneous distribution. Next, the suspension was dropped into a CaCl_2 solution (30 mL, 0.2 M) using a hypodermic needle (0.90 mm external diameter, 40 mm length). After stirring to cross-link for 10 min, the beads were washed for 10 min with H_2O to remove excess CaCl_2 .

3.2.2. Preparation of Chitosan-Coated Calcium Alginate Beads containing Catalyst/s

Beads were prepared according to previously reported procedure [55]: Pig liver esterase (270 U, 15 mg) was dissolved in H_2O (1.25 mL) and supplemented with sodium alginate solution (1.25 mL, 4% *w/w* in H_2O) to obtain a sodium alginate concentration of 2%. For experiments requiring co-encapsulated catalysts, Grubbs' catalyst (6.25 μmol , 5.31 mg or 25 μmol , 21.22 mg) was added. To reduce the particle size of non-water-soluble Grubbs' catalyst, the catalyst particle aggregates were crushed with a spatula, before stirring the suspension at 500 rpm for 10 min at room temperature for homogenisation. Then, the solution was dropped into a solution of chitosan (low molecular weight, 7.5 mL, 2% *w/w* in 1% acetic acid), CaCl_2 solution (7.5 mL, 0.4 M) and H_2O (15 mL) using a hypodermic needle (0.55 mm external diameter, 25 mm length). After stirring to cross-link for 10 min, the beads were titrated with NaOH (0.2 M) to remove excess CaCl_2 and neutralise remaining acetic acid.

3.2.3. Preparation of Multicompartment Beads made of Chitosan and Alginate Amide containing Pig Liver Esterase and Grubbs' Catalyst

First, the chitosan core was prepared according to previously reported procedure [55]: Pig liver esterase (270 U, 15 mg for standard amount of enzyme, 108 U, 6 mg for reduced amount of enzyme) was dissolved in chitosan solution (low molecular weight, 2% *w/w* in 1% acetic acid and 0.2 M CaCl_2 , 2.5 mL for beads with three shell layers, 1.0 mL for beads with five shell layers, 0.5 mL for beads with seven and twelve shell layers) and stirred for 10 min. Then, the solution (for twelve shell layers only one chitosan bead was produced) was dropped into a solution of sodium alginate (30 mL, 0.8% *w/w* in H_2O) using a hypodermic needle (0.55 mm external diameter, 25 mm length) and stirred for 5 min to build an approx. 0.5 mm thick calcium alginate coating. The beads were stirred for 5 min, before they were titrated with NaOH (0.2 M) to remove excess CaCl_2 and neutralise remaining acetic acid. To obtain cross-linked chitosan, the beads were added to a solution of glutaraldehyde (11.6 mL, 1% *v/v* in H_2O). After stirring for 20 h, the yellowish to brown coloured beads were extensively washed with H_2O . Next, the calcium alginate shell was dissolved by stirring the beads for 1 h in dissolving solution (30 mL, 15 mM citric acid, 25 mM Na_2CO_3). After washing the beads with H_2O , they were stirred in CaCl_2 solution (0.2 M) for 5 min and subsequently dried superficially on tissue paper. To apply the Grubbs' catalyst, the beads were rolled in catalyst powder. Then, the beads were added to an octyl-grafted alginate amide solution (30 mL, 0.8% *w/w* in H_2O) and stirred for 5 min for building an alginate amide shell. After briefly washing the beads with H_2O , they were stirred in CaCl_2 solution (0.2 M) for 5 min to ensure proper gelation of the shell and sufficient Ca^{2+} concentration for building the subsequent shell, starting by rolling the beads in Grubbs' catalyst powder. This procedure was then repeated until the desired quantity of layers was applied, and the specific amount of Grubbs' catalyst (25 μmol , 21.22 mg) was encapsulated. Before starting the reaction, the beads were stirred in H_2O -*t*BuOH (4:1) for 10 min to ensure the same medium condition inside the beads as in the reaction medium.

3.3. Reaction Procedures

3.3.1. Enzymatic Ester Hydrolysis Reaction Procedure

In a 15 mL glass vessel, non-encapsulated enzyme (270 U, 15 mg) or chitosan-coated alginate beads (2.5 g) containing PLE was/were suspended in 12.5 mL solvent. To start the reaction, diethyl cyclopent-3-ene-1,1-dicarboxylate (**2**) (0.25 mmol, 53 mg) was added and the reaction mixture was stirred at room temperature. Reaction rates including conversions of substrate **1** and pH compensation were measured respectively controlled by an automated titration with NaOH solution (0.2 M).

3.3.2. Tandem Chemoenzymatic Reaction Sequence Procedure

In a glass vessel, beads containing Grubbs' catalyst and PLE or the non-encapsulated catalysts were suspended in 12.5 mL (25 mL for specific experiments with a higher amount of bead material: Table 2, entries 6–8) H₂O/*t*BuOH (4:1). To start the reaction, diethyl cyclopent-3-ene-1,1-dicarboxylate (**2**) (0.25 mmol, 53 mg) was added and the reaction mixture was stirred at room temperature. Reaction rates, including conversions of substrate **1** and pH compensation, were measured respectively controlled by an automated titration with NaOH solution (0.2 M).

4. Conclusions

In summary, we successfully conducted a chemoenzymatic one-pot process combining a metathesis and enzymatic hydrolysis reaction in a tandem mode with catalysts being encapsulated in biopolymer hydrogel beads. Furthermore, multicompartment beads with a core-shell-design were created with catalysts located in different compartments. With this approach we addressed the issue of side product formation by creating beads with a larger diameter to enhance the diffusion route within the Grubbs' catalyst-containing shell, thus enhancing the selectivity from 1% to 75% towards the desired product. To improve selectivity and allow an increase in the enzymatic reaction rate, the substitution of crude PLE by PLE isoenzymes should be investigated in further optimised bead designs. Nevertheless, this proof of concept study contributes to developing chemoenzymatic reaction pathways using encapsulated catalysts and addressing reaction-related issues by designing specific immobilisates.

Supplementary Materials: The following are available online at <http://www.mdpi.com/2073-4344/9/6/547/s1>, Figure S1: ¹H NMR spectrum of octyl-grafted alginate amide, Figure S2: ¹H NMR spectrum of diethyl cyclopent-3-ene-1,1-dicarboxylate (**2**), Figures S3–S11: Calibration with 10–90% substance **3**, Figure S12: Calibration graph for determining the amount of substance **3**, Figure S13: Exemplary chromatogram for determination of selectivity, Table S1: Values for calibration of substance **3**, Table S2: Exemplary calculation of selectivity.

Author Contributions: Conceptualisation, J.P., H.G. and A.V.P.; methodology, J.P., H.G. and A.V.P.; investigation, J.P.; writing—original draft preparation, J.P. with the assistance of H.G. and A.V.P.; writing—review and editing, J.P., H.G. and A.V.P.; visualisation, J.P.; supervision, H.G. and A.V.P.

Funding: This Article is funded by the Open Access Publication Fund of Bielefeld University of Applied Sciences and the Deutsche Forschungsgemeinschaft (DFG, German Research Foundation)—414001623.

Conflicts of Interest: The authors declare no conflict of interest. The funders had no role in the design of the study; in the collection, analyses, or interpretation of data; in the writing of the manuscript, or in the decision to publish the results.

Appendix A

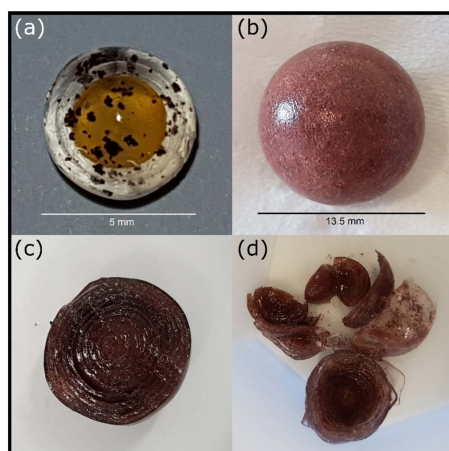


Figure A1. Multicompartment beads with PLE located inside the chitosan core and Grubbs' catalyst located in the octyl-grafted alginate amide shell: (a) three shell layers of alginate amide with Grubbs' catalyst non-crushed, (b) twelve shell layers of alginate amide with crushed Grubbs' catalyst for particle size reduction, (c) cross-section of twelve-layer-bead, (d) detached layers from the cut twelve-layer bead.

References

1. Anastas, P.T. Beyond reductionist thinking in chemistry for sustainability. *Trends Chem.* **2019**, *1*, 145–148. [[CrossRef](#)]
2. Erythropel, H.C.; Zimmerman, J.B.; de Winter, T.M.; Petitjean, L.; Melnikov, F.; Lam, C.H.; Lounsbury, A.W.; Mellor, K.E.; Janković, N.Z.; Tu, Q.; et al. The Green ChemisTREE: 20 years after taking root with the 12 principles. *Green Chem.* **2018**, *20*, 1929–1961. [[CrossRef](#)]
3. Kitanosono, T.; Masuda, K.; Xu, P.; Kobayashi, S. Catalytic organic reactions in water toward sustainable society. *Chem. Rev.* **2018**, *118*, 679–746. [[CrossRef](#)] [[PubMed](#)]
4. Shende, V.S.; Saptal, V.B.; Bhanage, B.M. Recent advances utilized in the recycling of homogeneous catalysis. *Chem. Rec.* **2019**. [[CrossRef](#)]
5. Sheldon, R.A. Fundamentals of green chemistry: Efficiency in reaction design. *Chem. Soc. Rev.* **2012**, *41*, 1437–1451. [[CrossRef](#)] [[PubMed](#)]
6. Sheldon, R.A.; Woodley, J.M. Role of Biocatalysis in Sustainable Chemistry. *Chem. Rev.* **2018**, *118*, 801–838. [[CrossRef](#)] [[PubMed](#)]
7. Drauz, K.; Gröger, H.; May, O. *Enzyme Catalysis in Organic Synthesis*; Wiley-VCH Verlag GmbH & Co. KGaA: Weinheim, Germany, 2012; ISBN 9783527639861.
8. Gandomkar, S.; Źadło-Dobrowolska, A.; Kroutil, W. Extending designed linear biocatalytic cascades for organic synthesis. *ChemCatChem* **2018**, *11*, 225–243. [[CrossRef](#)]
9. Rudroff, F.; Mihovilovic, M.D.; Gröger, H.; Snajdrova, R.; Iding, H.; Bornscheuer, U.T. Opportunities and challenges for combining chemo- and biocatalysis. *Nat. Catal.* **2018**, *1*, 12–22. [[CrossRef](#)]
10. Schmidt, S.; Castiglione, K.; Kourist, R. Overcoming the incompatibility challenge in chemoenzymatic and multi-catalytic cascade reactions. *Chem. Eur. J.* **2018**, *24*, 1755–1768. [[CrossRef](#)] [[PubMed](#)]
11. Gröger, H.; Hummel, W. Combining the ‘two worlds’ of chemocatalysis and biocatalysis towards multi-step one-pot processes in aqueous media. *Curr. Opin. Chem. Biol.* **2014**, *19*, 171–179. [[CrossRef](#)] [[PubMed](#)]
12. Wang, Y.; Zhao, H. Tandem reactions combining biocatalysts and chemical catalysts for asymmetric synthesis. *Catalysts* **2016**, *6*, 194. [[CrossRef](#)]
13. Denard, C.A.; Hartwig, J.F.; Zhao, H. Multistep one-pot reactions combining biocatalysts and chemical catalysts for asymmetric synthesis. *ACS Catal.* **2013**, *3*, 2856–2864. [[CrossRef](#)]
14. Ríos-Lombardía, N.; García-Álvarez, J.; González-Sabín, J. One-pot combination of metal- and bio-catalysis in water for the synthesis of chiral molecules. *Catalysts* **2018**, *8*, 75. [[CrossRef](#)]
15. Koszelewski, D.; Borys, F.; Brodzka, A.; Ostaszewski, R. Synthesis of enantiomerically pure 5,6-dihydropyran-2-ones via chemoenzymatic sequential DKR-RCM reaction. *Eur. J. Org. Chem.* **2019**, *2019*, 1653–1658. [[CrossRef](#)]
16. Makkee, M.; Kieboom, A.P.G.; van Bekkum, H.; Roels, J.A. Combined action of enzyme and metal catalyst, applied to the preparation of D-mannitol. *J. Chem. Soc. Chem. Commun.* **1980**, 930. [[CrossRef](#)]
17. Gomez Baraibar, A.; Reichert, D.; Mugge, C.; Seger, S.; Gröger, H.; Kourist, R. A one-pot cascade reaction combining an encapsulated decarboxylase with a metathesis catalyst for the synthesis of bio-based antioxidants. *Angew. Chem. Int. Ed.* **2016**, *55*, 14823–14827. [[CrossRef](#)] [[PubMed](#)]
18. Denard, C.A.; Bartlett, M.J.; Wang, Y.; Lu, L.; Hartwig, J.F.; Zhao, H. Development of a one-pot tandem reaction combining ruthenium-catalyzed alkene metathesis and enantioselective enzymatic oxidation to produce aryl epoxides. *ACS Catal.* **2015**, *5*, 3817–3822. [[CrossRef](#)]
19. Heidlindemann, M.; Rulli, G.; Berkessel, A.; Hummel, W.; Gröger, H. Combination of asymmetric organo- and biocatalytic reactions in organic media using immobilized catalysts in different compartments. *ACS Catal.* **2014**, *4*, 1099–1103. [[CrossRef](#)]
20. Suljić, S.; Pietruszka, J.; Worgull, D. Asymmetric bio- and organocatalytic cascade reaction - laccase and secondary amine-catalyzed α -arylation of aldehydes. *Adv. Synth. Catal.* **2015**, *357*, 1822–1830. [[CrossRef](#)]
21. Simon, R.C.; Busto, E.; Schrittwieser, J.H.; Sattler, J.H.; Pietruszka, J.; Faber, K.; Kroutil, W. Stereoselective synthesis of γ -hydroxynorvaline through combination of organo- and biocatalysis. *Chem. Commun.* **2014**, *50*, 15669–15672. [[CrossRef](#)]
22. Paris, J.; Ríos-Lombardía, N.; Morís, F.; Gröger, H.; González-Sabín, J. Novel insights into the combination of metal- and biocatalysis: Cascade one-pot synthesis of enantiomerically pure biaryl alcohols in deep eutectic solvents. *ChemCatChem* **2018**, *10*, 4417–4423. [[CrossRef](#)]

23. Bäckvall, J.-E.; Gustafson, K.; Görbe, T.; de Gonzalo, G.; Yang, N.; Schreiber, C.; Shchukarev, A.; Tai, C.-W.; Persson, I.; Zou, X. Chemoenzymatic dynamic kinetic resolution of primary benzylic amines using Pd(0)-CalB CLEA as a biohybrid catalyst. *Chemistry* **2019**. [[CrossRef](#)] [[PubMed](#)]
24. Gimbernat, A.; Guehl, M.; Lopes Ferreira, N.; Heuson, E.; Dhulster, P.; Capron, M.; Dumeignil, F.; Delcroix, D.; Girardon, J.; Froidevaux, R. From a sequential chemo-enzymatic approach to a continuous process for HMF production from glucose. *Catalysts* **2018**, *8*, 335. [[CrossRef](#)]
25. Ríos-Lombardía, N.; Vidal, C.; Liardo, E.; Morís, F.; García-Álvarez, J.; González-Sabín, J. From a sequential to a concurrent reaction in aqueous medium: Ruthenium-catalyzed allylic alcohol isomerization and asymmetric bioreduction. *Angew. Chem. Int. Ed.* **2016**, *55*, 8691–8695. [[CrossRef](#)] [[PubMed](#)]
26. Scalacci, N.; Black, G.W.; Mattedi, G.; Brown, N.L.; Turner, N.J.; Castagnolo, D. Unveiling the biocatalytic aromatizing activity of monoamine oxidases MAO-N and 6-HDNO: Development of chemoenzymatic cascades for the synthesis of pyrroles. *ACS Catal.* **2017**, *7*, 1295–1300. [[CrossRef](#)]
27. Simons, C.; Hanefeld, U.; Arends, I.W.C.E.; Maschmeyer, T.; Sheldon, R.A. Towards catalytic cascade reactions: Asymmetric synthesis using combined chemo-enzymatic catalysts. *Top. Catal.* **2006**, *40*, 35–44. [[CrossRef](#)]
28. Sperl, J.M.; Carsten, J.M.; Guterl, J.-K.; Lommes, P.; Sieber, V. Reaction design for the compartmented combination of heterogeneous and enzyme catalysis. *ACS Catal.* **2016**, *6*, 6329–6334. [[CrossRef](#)]
29. Edwards, E.; Roychoudhury, R.; Schwarz, B.; Jordan, P.; Lisher, J.; Uchida, M.; Douglas, T. Co-localization of catalysts within a protein cage leads to efficient photochemical NADH and/or hydrogen production. *J. Mater. Chem. B* **2016**, *4*, 5375–5384. [[CrossRef](#)]
30. Patterson, D.; Edwards, E.; Douglas, T. Hybrid nanoreactors: Coupling enzymes and small-molecule catalysts within virus-like particles. *Isr. J. Chem.* **2015**, *55*, 96–101. [[CrossRef](#)]
31. Rulli, G.; Heidlindemann, M.; Berkessel, A.; Hummel, W.; Gröger, H. Towards catalyst compartmentation in combined chemo- and biocatalytic processes: Immobilization of alcohol dehydrogenases for the diastereoselective reduction of a β -hydroxy ketone obtained from an organocatalytic aldol reaction. *J. Biotechnol.* **2013**, *168*, 271–276. [[CrossRef](#)]
32. Tosa, T.; Mori, T.; Fuse, N.; Chibata, I. Studies on continuous enzyme reactions. I. Screening of carriers for preparation of water-insoluble aminoacylase. *Enzymologia* **1966**, *31*, 214–224.
33. Cacicedo, M.L.; Manzo, R.M.; Municoy, S.; Bonazza, H.L.; Islan, G.A.; Desimone, M.; Bellino, M.; Mammarella, E.J.; Castro, G.R. Immobilized enzymes and their applications. In *Advances in Enzyme Technology*, 1st ed.; Singh, R.S., Singhania, R.R., Pandey, A., Larroche, C., Eds.; Elsevier: Amsterdam, The Netherlands, 2019; pp. 169–200. ISBN 9780444641144.
34. Sheldon, R.A.; van Pelt, S. Enzyme immobilisation in biocatalysis: Why, what and how. *Chem. Soc. Rev.* **2013**, *42*, 6223–6235. [[CrossRef](#)] [[PubMed](#)]
35. Kierstan, M.; Bucke, C. The immobilization of microbial cells, subcellular organelles, and enzymes in calcium alginate gels. *Biotechnol. Bioeng.* **1977**, *19*, 387–397. [[CrossRef](#)] [[PubMed](#)]
36. Von Langermann, J.; Wapenhensch, S. hydroxynitrile lyase-catalyzed synthesis of enantiopure cyanohydrins in Biocatalytic Active Static Emulsions (BASE) with suppression of the non-enzymatic side reaction. *Adv. Synth. Catal.* **2014**, *356*, 2989–2997. [[CrossRef](#)]
37. Haque, R.U.; Paradisi, F.; Allers, T. Haloferax volcanii as immobilised whole cell biocatalyst: New applications for halophilic systems. *Appl. Microbiol. Biot.* **2019**, *103*, 3807–3817. [[CrossRef](#)] [[PubMed](#)]
38. Planchestainer, M.; Roura Padrosa, D.; Contente, M.L.; Paradisi, F. Genetically fused T4L acts as a shield in covalent enzyme immobilisation enhancing the rescued activity. *Catalysts* **2018**, *8*, 40. [[CrossRef](#)]
39. De Andrades, D.; Graebin, N.G.; Kadowaki, M.K.; Ayub, M.A.Z.; Fernandez-Lafuente, R.; Rodrigues, R.C. Immobilization and stabilization of different β -glucosidases using the glutaraldehyde chemistry: Optimal protocol depends on the enzyme. *Int. J. Biol. Macromol.* **2019**, *129*, 672–678. [[CrossRef](#)]
40. Saha, S.; Pal, A.; Kundu, S.; Basu, S.; Pal, T. Photochemical green synthesis of calcium-alginate-stabilized Ag and Au nanoparticles and their catalytic application to 4-nitrophenol reduction. *Langmuir* **2010**, *26*, 2885–2893. [[CrossRef](#)]
41. Primo, A.; Liebel, M.; Quignard, F. Palladium coordination biopolymer: A versatile access to highly porous dispersed catalyst for suzuki reaction. *Chem. Mater.* **2009**, *21*, 621–627. [[CrossRef](#)]

42. Harrad, M.A.; Boualy, B.; El Firdoussi, L.; Mehdi, A.; Santi, C.; Giovagnoli, S.; Nocchetti, M.; Ait Ali, M. Colloidal nickel(0)-carboxymethyl cellulose particles: A biopolymer-inorganic catalyst for hydrogenation of nitro-aromatics and carbonyl compounds. *Catal. Commun.* **2013**, *32*, 92–100. [[CrossRef](#)]
43. Veisi, H. Efficient cyanation of aryl halides with $K_4[Fe(CN)_6]$ catalyzed by encapsulated palladium nanoparticles in biguanidine–chitosan matrix as core–shell recyclable heterogeneous nanocatalyst. *Polyhedron* **2019**, *159*, 212–216. [[CrossRef](#)]
44. Anku, W.W.; Oppong, S.O.-B.; Shukla, S.K.; Agorku, E.S.; Govender, P.P. Chitosan–sodium alginate encapsulated Co-doped ZrO_2 –MWCNTs nanocomposites for photocatalytic decolorization of organic dyes. *Res. Chem. Intermed.* **2016**, *42*, 7231–7245. [[CrossRef](#)]
45. Pauly, J.; Gröger, H.; Patel, A.V. Catalysts encapsulated in biopolymer hydrogels for chemoenzymatic one-pot processes in aqueous media. *ChemCatChem* **2019**, *11*, 1504–1510. [[CrossRef](#)]
46. Tenbrink, K.; Seßler, M.; Schatz, J.; Gröger, H. Combination of olefin metathesis and enzymatic ester hydrolysis in aqueous media in a one-pot synthesis. *Adv. Synth. Catal.* **2011**, *353*, 2363–2367. [[CrossRef](#)]
47. Pauly, J.; Gröger, H.; Patel, A.V. Metathesis in water conducted by tailor-made encapsulated Grubbs' catalyst. *Green Chem.* **2018**, *20*, 5179–5187. [[CrossRef](#)]
48. Schneider, M.; Engel, N.; Boensmann, H. Enzymatic syntheses of chiral building blocks from racemates: Preparation of (1R,3R)-chrysanthemic, -permethrinic and -caronic acids from racemic, diastereomeric mixtures. *Angew. Chem. Int. Ed. Engl.* **1984**, *23*, 64–66. [[CrossRef](#)]
49. Domínguez de María, P.; Kossmann, B.; Potgrave, N.; Buchholz, S.; Trauthwein, H.; May, O.; Gröger, H. Improved Process for the Enantioselective Hydrolysis of Prochiral Diethyl Malonates Catalyzed by Pig Liver Esterase. *Synlett* **2005**, 1746–1748. [[CrossRef](#)]
50. Junge, W.; Heymann, E. Characterization of the isoenzymes of pig-liver esterase 2. kinetic studies. 2. kinetic studies. *Eur. J. Biochem.* **1979**, *95*, 519–525. [[CrossRef](#)]
51. Öhrner, N.; Mattson, A.; Norin, T.; Hult, K. Enantiotopic selectivity of-pig liver esterase isoenzymes. *Biocatalysis* **2009**, *4*, 81–88. [[CrossRef](#)]
52. Tamm, C. Pig liver esterase catalyzed hydrolysis: Substrate specificity and stereoselectivity. *Pure Appl. Chem.* **1992**, *64*, 1187–1191. [[CrossRef](#)]
53. Lam, L.K.P.; Brown, C.M.; de Jeso, B.; Lym, L.; Toone, E.J.; Jones, J.B. Enzymes in organic synthesis. 42. Investigation of the effects of the isozymal composition of pig liver esterase on its stereoselectivity in preparative-scale ester hydrolysis of asymmetric synthetic value. *J. Am. Chem. Soc.* **1988**, *110*, 4409–4411. [[CrossRef](#)]
54. Hummel, A.; Brüsehauer, E.; Böttcher, D.; Trauthwein, H.; Doderer, K.; Bornscheuer, U.T. Isoenzymes of pig-liver esterase reveal striking differences in enantioselectivities. *Angew. Chem. Int. Ed.* **2007**, *46*, 8492–8494. [[CrossRef](#)] [[PubMed](#)]
55. Pauly, J.; Gröger, H.; Patel, A.V. Design, characterisation and application of alginate-based encapsulated pig liver esterase. *J. Biotechnol.* **2018**, *280*, 42–48. [[CrossRef](#)] [[PubMed](#)]
56. Hu, W.; Li, J.; Hou, H.; Yan, H.; Feng, Y.; Mi, X.; Lin, Q. Preparation and characterization of hydrophobic alginate derivative nanocapsules entrapping l-Cyhalothrin. *Asian J. Chem.* **2013**, *25*, 9904–9908. [[CrossRef](#)]

